Structural and Functional Models of the Dimanganese Catalase Enzymes. 3. Kinetics and Mechanism of Hydrogen Peroxide Dismutation

P. J. Pessiki and G. C. Dismukes*

Contribution from the Princeton University, Department of Chemistry, Henry H. Hoyt Laboratory, Princeton, New Jersey 08544

Received July 16, 1993®

Abstract: The mechanism of peroxide dismutation by synthetic mimics of the dimanganese catalase enzymes has been investigated by steady-state kinetic methods. These compounds, $[LMn_2^{II,II}(\mu\text{-}X)](ClO_4)_2$, $X^- = CH_3CO_2^-$ and $ClCH_2CO_2^-$, were found to share structural, redox, and spectroscopic properties analogous to the catalase enzymes (Pessiki et al. *J. Am. Chem. Soc.* preceding paper in this issue). The dismutation mechanism proceeds by two consecutive two-electron steps: $H_2O_2 + 2e^- + 2H^+ \rightarrow 2H_2O$ and $H_2O_2 \rightarrow O_2 + 2e^- + 2H^+$ which are coupled to redox transformation of the catalyst: $Mn_2^{III,III} \leftrightarrow Mn_2^{II,II}$. The μ-carboxylate derivatives are inactive, but in the presence of water they autocatalytically dismutate H_2O_2 after an initial hydration reaction in which the μ-carboxylate ligand appears to dissociate, as judged by inhibition with acetate. The observed steady-state rate expression, $\nu(O_2) = k_{obs}[H_2O_2]^1$-$[(LMn_2(CH_3CO_2)(ClO_4)_2]$,[1] $k_{obs} = 0.23\ M^{-1}\ s^{-1}$, exhibits the same molecularities with respect to peroxide and catalyst as observed for the enzyme from *T. thermophilus*, for which k_{obs} is 10^7 faster. In contrast, the rate law for the μ-Cl^- derivative, LMn_2Cl_3, is second order in $[H_2O_2]$ (Mathur et al. *J. Am. Chem. Soc.* **1987**, *109*, 5227). EPR and optical studies support a mechanism involving oxidation to a $Mn_2^{III,III}$ intermediate and against formation of the mixed valence states, $Mn_2^{II,III}$ and $Mn_2^{III,IV}$. The rate-limiting step for the model complexes is ascribed to either the inner-sphere two-electron intramolecular oxidation of the peroxide complex, $[LMn_2^{II,II}(H_2O_2)]^{3+} \rightarrow [LMn_2^{III,III}(OH)_2]^{3+}$, or a proton dissociation reaction coupled to this oxidation. Subsequent two-electron reduction to the $Mn_2^{II,II}$ oxidation state via a second H_2O_2 molecule occurs 7-9-fold faster and completes the catalytic cycle. The 10^7 faster rate for the enzyme is proposed to reflect either a substantially lower reduction potential for the $MnCat^{III,III}$ oxidation state, the availability of active site residues which function as proton donors and acceptors, or both.

Introduction

Hydrogen peroxide is readily formed in all aerobic cells by reduction of dioxygen and superoxide. The molecule is extremely toxic to living cells owing to oxidative damage. It has been linked to a variety of pathological consequences, including aging, ischemia, diabetes, and cancer.[1] Both prokaryotes and eukaryotes have evolved defense mechanisms to cope with its unavoidable formation. Among these are the catalase enzymes which catalytically dismutate hydrogen peroxide.

Spectroscopic studies of the dimanganese catalase enzyme (MnCat) from *T. thermophilus*[2] and *L. plantarum*[3] have revealed a limited picture implicating two of the four accessible oxidation states, a "reduced" $Mn_2^{II,II}$ state, and an "oxidized" $Mn_2^{III,III}$, in the catalase mechanism (Scheme 1).[4] A catalytically inactive mixed valence "superoxidized" state, $Mn_2^{III,IV}$, can be quantitatively produced by oxidation with a variety of oxidants, including autoxidation in air (yielding only a minor amount). A second mixed valence "semioxidized" species, $Mn_2^{II,III}$, forms as a minority species by autoxidation in air or by reduction of the superoxidized species with iodide. It appears not to be involved in catalysis, although this has not been thoroughly investigated.

The rate-limiting first step in the catalytic cycle involves the bimolecular oxidation of the $Mn_2^{II,II}$ state by one molecule of peroxide to form an EPR silent species, with rate constant approaching $1 \times 10^7\ M^{-1}\ s^{-1}$ (reviewed in ref 4). The low steady-state concentration of this intermediate in the presence of peroxide has precluded a definitive analysis, although optical and EPR data suggest a spin-coupled $Mn_2^{III,III}$ oxidation state. A second peroxide molecule reduces this species to the $Mn_2^{II,II}$ state with release of O_2. Because the Mn-ligand coordination structures of the reduced and oxidized enzyme are not known, the structural basis for catalysis remains speculative. Those noted in Scheme 1 are based on chemically reasonable candidates. In particular, the nature of the bound peroxo intermediate is unclear; it could involve any of several possible bridging coordination modes for the peroxo ligand such as μ-$\eta^1\eta^1$, μ-$\eta^2\eta^0$, or possibly a μ-oxo species plus water. Peroxide coordination to a single Mn ion may also be possible. Examples of each of these may be found in the literature. For example, a stable μ-$\eta^1\eta^1$-peroxo-$Mn_2^{IV,IV}$ species

† Keywords: manganese, catalase, hydrogen peroxide, enzyme mechanism, kinetics.

‡ Abbreviations: MnCat, dimanganese catalase enzyme; LH, = *N,N,N',N'*-tetrakis(2-methylenebenzimidazole)-1,3-diaminopropan-2-ol.

® Abstract published in *Advance ACS Abstracts*, January 1, 1994.

(1) (a) *Oxidative Stress*; Sies, H., Ed.; Academic Press: London, 1985. (b) *Oxygen Radicals in Biology and Medicine*; Simic, M. G., Taylor, K. A., Ward, J. F., von Sonntag, C., Eds.; Plenum Press: New York, 1988. (c) *Medical, Biochemical and Chemical Aspects of Free Radicals*; Hayaishi, O., Niki, E., Kondo, M., Yoshikawa, Eds.; Elsevier: Amsterdam, 1990.

(2) (a) Khangulov, S. V.; Barynin, V. V.; Melik-Adamyan, V. R.; Grebenko, A. I.; Voevodskay, N. V.; Blumenfeld, L. A.; Dobrykov, S. N.; Il'ysova, V. B. *Bioorgan. Khimiya* **1986**, *12*, 741-748 (Russ.). (b) Khangulov, S. V.; Voyevodskaya, N. V.; Barynin, V. V.; Grebenko, A. I.; Melik-damyan, V. R. *Biofizika* **1987**, *32*, 1044-1051 (Engl.), 960-966 (Russ.). (c) Khangulov, S. V.; Barynin, V. V.; Antonyuk-Barynina, S. W. *Biochim. Biophys. Acta* **1990**, *1020*, 25-33. (d) Khangulov, S. V.; Barynin, V. V.; Voevodskaya, N. V.; Grebenko, A. I. *Biochim. Biophys. Acta* **1990**, *1020*, 305-310. (e) Khangulov, S. V.; Andreeva, N. E.; Gerasimenko, V. V.; Goldfeld, M. G.; Barynin, V. V.; Grebenko, A. I. *Russ. J. Phys. Chem.* **1990**, *64*, 10-16. (f) Khangulov, S. V.; Goldfeld, M. G.; Gerasimenko, V. V.; Andreeva, N. E.; Barynin, V. V.; Grebenko, A. I. *J. Inorg. Biochem.* **1990**, *40*, 279-292.

(3) (a) Penner-Hahn, J. E. In *Manganese Redox Enzymes*; Pecoraro, V. L., Ed.; Verlag Chemie: New York, 1992; pp 29-46. (b) Waldo, G. S.; Fronko, R. M.; Penner-Hahn, J. E. *Biochemistry* **1991**, *30*, 10486-10490. (c) Waldo, G. S.; Yu, S.; Penner-Hahn, J. E. *J. Am. Chem. Soc.* **1992**, *114*, 5869-5870.

(4) (a) Dismukes, G. C. Polynuclear Manganese Enzymes. In *Bioinorganic Catalysis*; Reedijk, J., Ed.; Marcel Dekker: Amsterdam, 1992. (b) Pessiki, P. J.; Khangulov, S. V.; Dismukes, G. C.; Barynin, V. V. In *Macromolecular Host-Guest Complexes: Optical, Optoelectronic and Photorefractive Properties and Applications*; Jenheke, S., Ed.; Materials Research Society: Pittsburgh, PA, 1992; Vol. 277, pp 75-86.

0002-7863/94/1516-0898$04.50/0

Scheme 1. Proposed Mechanism of the Catalysis of H_2O_2 Dismutation by Manganese Catalase

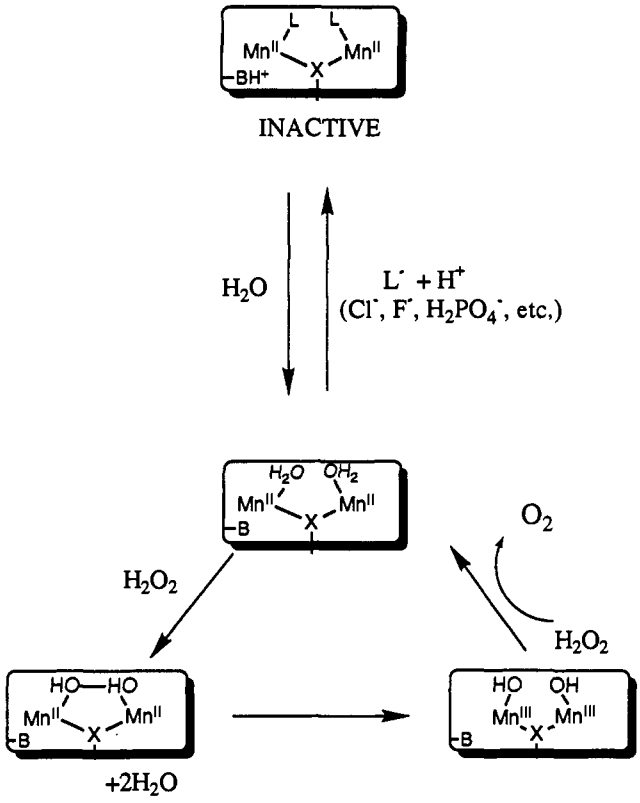

has been prepared synthetically as well as a trinuclear $Mn_3^{III,III,III}$ complex.[5] μ-Oxo bridge formation occurs upon oxidation in water for a variety of Mn dimers.[6,7] Also, oxidative coordination of dioxygen to a single Fe^{II} atom in the diiron site of hemerythrin has been established for these reversible O_2 binding proteins (reviewed in ref 7).

Why the catalase reaction does not occur using the two mixed valence states of the enzyme is less clear. ENDOR studies indicate that substrate accessibility within the superoxidized state is limited to a single solvent exchangeable site in the second solvation shell, which suggests a possible kinetic barrier.[8] EXAFS[3c] and EPR[9] studies indicate that this oxidation state has six-coordinate Mn ions and a di-μ-oxo bridge which defines the equatorial sites of the planar Mn_2O_2 rhombus. This structure tends to be slow to exchange equatorial ligands (oxo) for both Mn^{III} and Mn^{IV}.[4,6]

Another unexplained puzzle is why MnCat exhibits undetectable superoxide dismutase activity, corresponding to reversible one-electron oxidation and reduction of superoxide.[10]

The $Mn_2^{II,II}$ state of both the *T. thermophilus*[2a,b] and the *L. plantarum* enzymes[3a,b] undergoes facile ligand substitution reactions involving a variety of small anions (Cl^-, F^-, N_3^-, NO_3^-, $H_2PO_4^-$) with concomitant inhibition of catalase activity. Binding appears to take place directly to one or both Mn^{II} ion(s), as judged by the dependence of the zero-field splitting parameters observed by EPR.[2a,b] In the case of Cl^-, between pH 10 and 6 where both the enzyme activity is independent of pH and Cl^- is not protonated in solution, inhibition requires uptake of one proton/Cl. This indicates that proton binding (or hydroxide dissociation) accompanies or preceeds the binding of the anion inhibitors at the active site.

Here we address these questions using new derivatives[4b,11] of a synthetic dimanganese model of MnCat, **1**, to investigate the structural basis for the enzyme's Mn oxidation state preference, inhibition by anions and the high catalase rate. Moreover, we have found that the μ-carboxylate derivatives of **1** are more stable against dissociation of Mn^{II} and are considerably more soluble in polar solvents compared to the halide derivatives, LMn_2Cl_3 and $LMn_2(OH)Br_2$.[12] The improved solubility has greatly simplified mechanistic studies by enabling dissolution of both reactant and catalyst in a single homogeneous phase. This has revealed a different molecularity for peroxide in the rate-limiting step of dismutation by **1** than is observed with LMn_2Cl_3, which is in agreement with the rate-limiting step in catalysis by MnCat.

Structure 1 :$[LMn_2(II,II)(\mu\text{-}CH_3CO_2)](ClO_4)_2$,

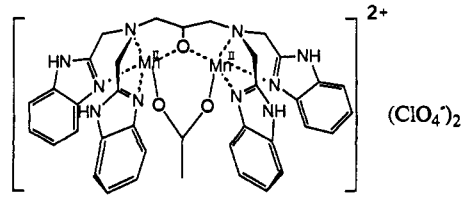

Experimental Methods

The time course of oxygen concentration was determined polarographically using a Clark type electrode (YSI, Yellow Springs). The limiting time constant was 1 s. All reactions were done anaerobically in degassed methanol or acetonitrile. The hydrogen peroxide solutions were made from 30% aqueous solutions diluted in methanol; concentration was verified by absorption at 230 nm using $\epsilon = 60\ cm^{-1}\ M^{-1}$. The order of addition of the reactants had no consequence on the measured rate of oxygen production.

The Clark electrode method is a significant advantage over our previous manometric study employing LMn_2Cl_3. Owing to the need to accumulate detectable volumes of O_2 gas, this method was restricted to slow kinetics where steady-state behavior had been reached. The electrode method allows data collection in the pre-steady-state region. Also, owing to insolubility of LMn_2Cl_3 in polar solvents suitable for H_2O_2, this compound required a two-phase solvent system for catalase activity studies. The current results obtained on **1** in a single homogeneous phase differ in terms of H_2O_2 molecularity from those obtained on LMn_2Cl_3 in a two phase system.

EPR and UV. Instruments and conditions are noted in the preceding paper in this issue.[11]

Results

Catalase Activity. The catalase reaction is autocatalytic. Addition of excess aqueous H_2O_2 to a methanol solution of **1** produces no O_2 initially, but this grows in exponentially in time, reaching a steady-state which continues undiminished until the peroxide is consumed. Following this, subsequent addition of peroxide restores the steady-state rate again, but without the lag phase. We investigated the dependence of the lag time and steady-state O_2 production rate on the concentration of water and excess acetate.

Acetate Inhibition. Addition of tetra-*n*-ethylammonium acetate to the reaction mixture decrease the steady-state rate of O_2 production, as summarized in Table 1. About a 4-fold reduction in the rate could be affected by a 20-fold excess of acetate over

(5) (a) Bhula, R.; Gainsford, G. J.; Weatherburn, D. C. *J. Am. Chem. Soc.* **1988**, *110*, 7550–7552. (b) Bossek, U.; Weyhermuller, T.; Wieghardt, K.; Nuber, B.; Weiss, J. *J. Am. Chem. Soc.* **1990**, *112*, 6387–6388.

(6) (a) Wieghardt, K.; Bossek, U.; Bonvoisin, J.; Beauvillain, P.; Girerd, J.-J.; Nuber, B.; Weiss, J.; Heinze, J. *Angew. Chem., Int. Ed. Engl.* **1986**, *25*, 1030–1034. (b) Sheats, J. E.; Czernuziewicz, R.; Dismukes, G. C.; Rheingold, A.; Petrouleas, V.; Stubbe, J.; Armstrong, W. H.; Beer, R.; Lippard, S. J. *J. Am. Chem. Soc.* **1987**, *109*, 1435–1444.

(7) Que, L.; True, A. *Prog. Inorg. Chem.* **1990**, *38*, 97–200.

(8) Khangulov, S. V.; Sivaraja, M.; Barynin, V. V.; Dismukes, G. C. *Biochemistry* **1993**, *32*, 4912–4924.

(9) Zheng, M.; Khangulov, S. V.; Dismukes, G. C.; Barynin, V. V. *Inorg. Chem.* In press.

(10) Beyer, W. F.; Fridovich, I. In *Oxygen Radicals in Biology and Medicine*: *Basic-Life Sciences*; Simic, M. G., Taylor, K. A., Ward, J. F., von Sonntag, C., Eds.; Plenum Press: New York, 1988; pp 651–661.

(11) Pessiki, P. J.; Khangulov, S. V.; Ho, D. M.; Dismukes, G. C. *J. Am. Chem. Soc.*, preceding article in this issue.

(12) (a) Mathur, P.; Crowder, M.; Dismukes, G. C. *J. Am. Chem. Soc.* **1987**, *109*, 5227–5232.

Table 1. Steady-State Rate of Oxygen Formation from H_2O_2 as a Function of Tetra-*n*-ethylammonium Acetate Concentration[a]

[NR_4OAc], M	rate, mM O_2 s^{-1}
0.0 M	3.71×10^{-4}
1.0×10^{-3}	2.05×10^{-4}
2.0×10^{-3}	8.7×10^{-5}

[a] An active form of $[LMn_2CH_3CO_2](ClO_4)_2$ was used for this experiment (as described in text). $[LMn_2CH_3CO_2](ClO_4)_2$ concentration (1×10^{-4} M) and HOOH concentration (1×10^{-2} M) in methanol.

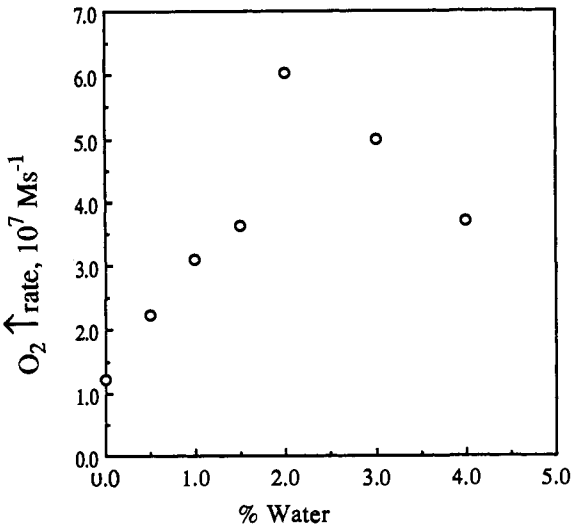

Figure 1. The rate of oxygen formation as a function of water content: $[LMn_2(CH_3CO_2)](ClO_4)_2$ concentration (1×10^{-4} M); H_2O_2 concentration (1×10^{-2} M), solvent is methanol.

catalyst. To obtain the results in Table 1 an active form of the reduced catalyst was used, obtained by allowing **1** to react initially with excess H_2O_2 until all the H_2O_2 is consumed.

Water as Reactant. Addition of a few percent water to a methanolic solution of the catalyst prior to addition of H_2O_2 reduces the initial lage phase for O_2 production and increases the steady-state rate. By holding both the concentration of H_2O_2 and catalyst constant the rate of O_2 production was measured as a function of water concentration. The data are graphed in Figure 1. Initially, the steady-state rate at which O_2 is produced increases by 5-fold as the water content is increased to 2%, followed by a decrease at greater water concentration. The initial lag time for O_2 production decreases by 50% in the 0–2% water range when added prior to peroxide and remains constant above 2% water.

Reactant Molecularity. The steady-state rate of O_2 production was found to be first-order in both catalyst and peroxide. Figure 2 presents a plot of the dependence of the rate on the concentration of $[LMn_2X]Y_2$, while the concentration of H_2O_2 is held constant. The linearity of the slope indicates an order of one for both $[LMn_2(CH_2CO_2)]Y_2$, Y = ClO_4^- and BPh_4^-, when extrapolated to low concentration of catalyst. At higher catalyst concentrations the apparent rate of O_2 production falls off; however, this appers to reflect the limited solubility of O_2 in the organic solvent when produced at these higher rates. Previous volumetric studies not limited by O_2 solubility found a first-order dependence on catalyst concentration at even higher concentrations.[12] The range for k_{obs} is 0.2–0.3 M^{-1} s^{-1}, in the concentration range of 0.005 to 0.04 mM for **1** using the observed steady-state rate expression, $\nu(O_2) = k_{obs}[H_2O_2]^1[(LMn_2(CH_3CO_2)(ClO_4)_2],^1$ with the average k_{obs} = 0.23 M^{-1} s^{-1}.

Figure 3 plots the dependence of the steady-state rate on the concentration of H_2O_2, while the concentration of catalyst is fixed. The linearity of the slope indicates an order of 1 for H_2O_2 in the rate expression up to at least 0.1 mM. This result contrasts with the reaction order of 2 for H_2O_2 obtained previously using LMn_2Cl_3 as the catalyst but by necessity using a two phase solvent system of butanol/water.[12]

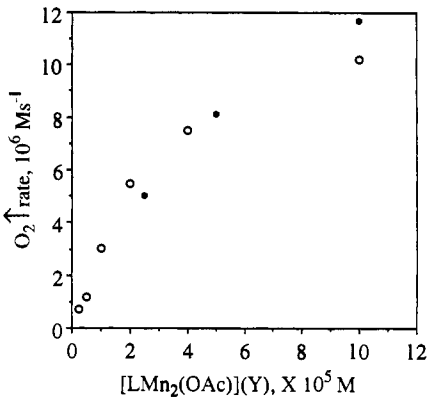

Figure 2. The rate of oxygen formation at constant H_2O_2 concn (1×10^{-2} M) and different catalyst concentrations $[LMn_2CH_3CO_2](Y)_2$: Y = ClO_4^- (open circles) and BPh_4^- (filled circles), solvent is methanol.

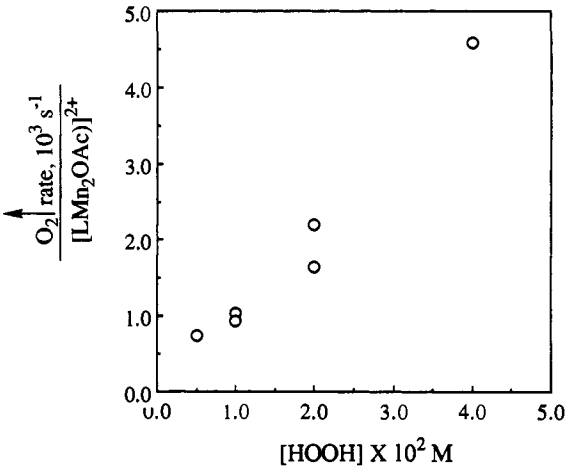

Figure 3. The rate of oxygen formation as a function of H_2O_2 concentration, solvent is methanol.

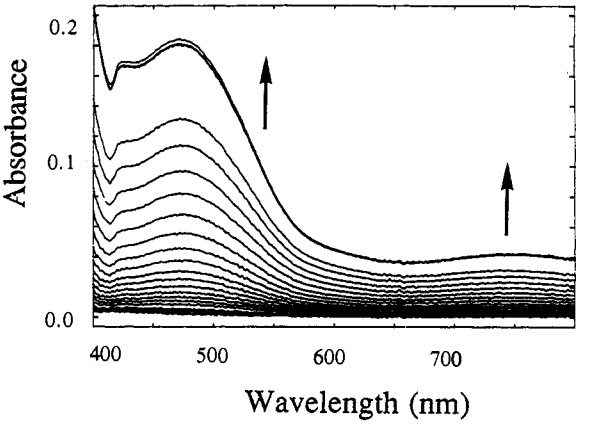

Figure 4. Time dependence of the visible absorption spectrum of a 1:1 mixture of $[LMn_2(CH_3CO_2)](ClO_4)_2$ and H_2O_2 in methanol: concentrations 2.5 mM each.

Catalytic Intermediates. Reaction of the colorless catalyst with a stoichiometric amount of H_2O_2 in methanol produces a colored species having the visible spectrum shown in Figure 4. It reveals three peaks at 425, 472, and 760 nm. The optical transitions are consistent with a Mn^{III} or $Mn_2^{III,III}$ species.[6] When the concentration of peroxide is less than or slightly greater than the concentration of catalyst the absorbance of the 472-nm band increases monotonically with time to a final maximum which is a linear function of the starting concentration of peroxide. This is the behavior expected if there is a single species formed. By

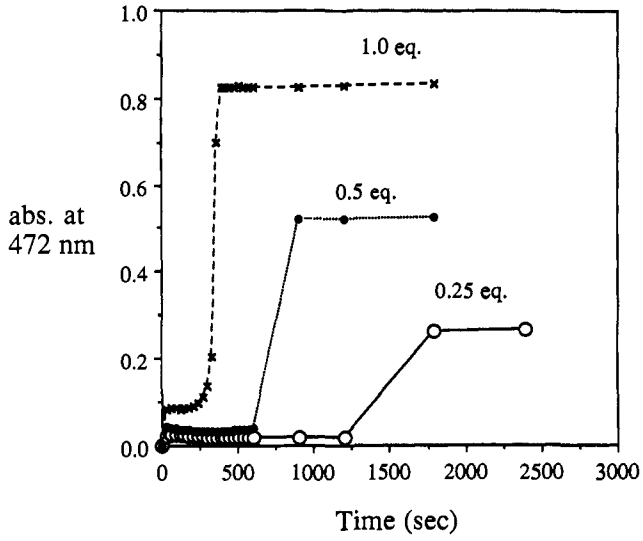

Figure 5. Plot of the time dependence of the absorbance at 472 nm at different $[LMn_2CH_3CO_2](ClO_4)_2$ concentrations (2.5, 1.25, and 0.625 mM) with H_2O_2 concentration held constant in methanol: $[H_2O_2]$ = 0.35 mM (140, 280 and 560 equiv).

contrast, when H_2O_2 is in large excess, a steady state is achieved much below the maximum absorbance and only at the end of the reaction does the absorbance increase. Figure 5 demonstrates this point. Thus any mechanism must account for the $Mn_2^{III,III}$ concentration in the steady-state reaction. Also, in Figure 5 the ratio of steady-state absorbance of $Mn_2^{III,III}$ to the initial $Mn_2^{II,II}$ concentration is found to be nearly constant (initial abs/[Cat] = 1.0, 0.9, 0.85). It also shows that the final absorbance reached after consumption of excess peroxide increases linearly with the initial concentration of catalyst (final abs/[Cat] = 1.04, 0.96, 0.83). The final absorbance level is reversibly bleached by the addition of more peroxide. This behavior indicates a stoichiometric reaction with peroxide forming an initial intermediate which can then react with excess peroxide in a faster reaction to achieve a lower steady-state concentration of the intermediate. The ratio of the final to steady-state absorbance changes in Figure 5 is 7–9:1, indicating a faster rate of destruction (reduction) of the intermediate than formation (oxidation).

The interaction of H_2O_2 with the catalyst was also monitored by low-temperature EPR spectroscopy. The reaction was performed in both CH_3CN and methanol solvents at room temperature and quenched by freezing in liquid nitrogen. The results of the reaction employing CH_3CN are shown in Figure 6. Once the reaction reaches steady state in 60 s there is a 49% decrease in the $Mn_2^{II,II}$ EPR signal intensity, and a minor amount of an uncoupled high symmetry Mn^{2+} species is formed. The latter species produces the six-line signal appearing at g = 2. We estimate the Mn^{2+} species to be much less than 5% of the $Mn_2^{II,II}$ species. At the end of the reaction the $Mn_2^{II,II}$ intensity is largely restored, and the Mn^{2+} signal disappears. The data in Figure 6 were recorded at a temperature of 50 K. Similar results are seen below 10 K. These results indicate that under conditions of steady-state turnover the $Mn_2^{II,II}$ species is converted to an EPR silent species and a small amount of uncoupled, i.e., monomeric, Mn^{2+} species which disappears at the end of the reaction or recouples to form the starting $Mn_2^{II,II}$ species. The leading candidates for the EPR silent species is a Mn^{III} monomer or $Mn_2^{III,III}$ dimer. These results are fully consistent with the optical data indicating reversible formation of a $Mn_2^{III,III}$ or monomeric Mn^{III} species in nearly all of the centers.

Addition of a small amount of water changes the initial EPR spectrum of the $Mn_2^{II,II}$ form of the catalyst, indicative of binding or reaction with water. The course of the reaction with peroxide in methanol is qualitatively the same as in acetonitrile but differs quantitatively in terms of the steady-state yield of intermediate.

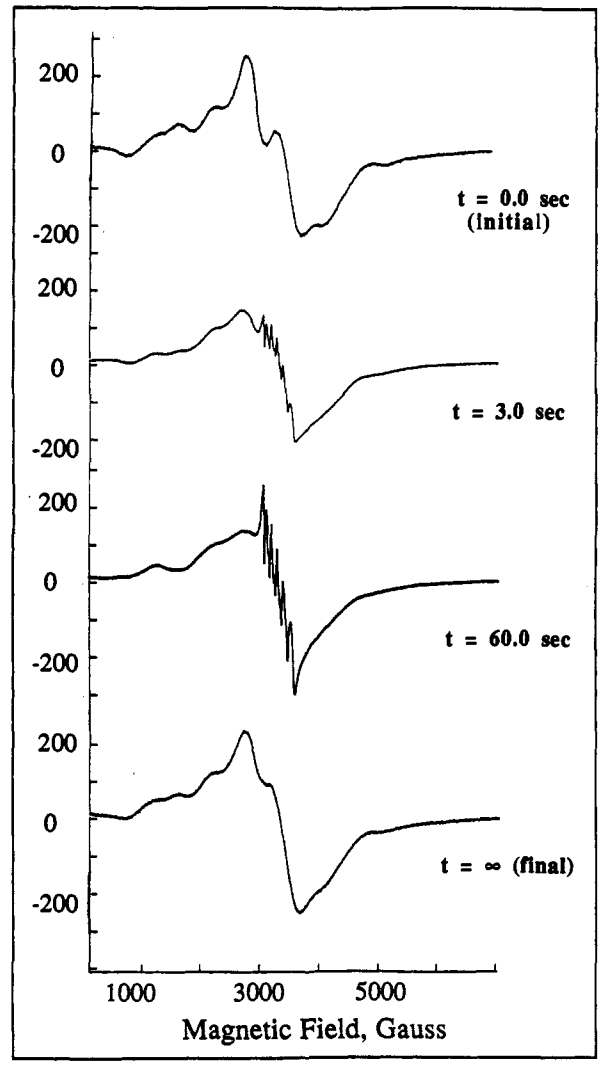

Figure 6. The reaction between H_2O_2 and $[LMn_2(CH_3CO_2)](ClO_4)_2$ monitored by EPR spectroscopy: conditions: T = 50 K, power = 10 mW, concentration = 1 mmolar, H_2O_2 = 0.6 M, solvent = CH_3CN.

As is also true in acetonitrile, an EPR silent colored species forms in the steady state. However, the steady-state yield is higher, indicating a larger yield of the oxidized species and a greater loss of the $Mn_2^{II,II}$ species. Also, at the end of the reaction with all peroxide consumed there is a greater conversion of the $Mn_2^{II,II}$ EPR spectrum to the EPR silent oxidized species than is observed in acetonitrile. This behavior is consistent with the optical data in Figure 5 showing that in methanol more of the catalyst is oxidized at the end of the reaction.

Superoxide Dismutase Activity. The SOD activity of 1 was examined by stopped-flow kinetic methods in solutions of 50–100 μM O_2^- at pH 7.3–8.1 by monitoring the absorbance change at 245 nm.[14] No detectable level of dismutation was observed indicating a maximum bimolecular rate constant less than 5×10^5 mol^{-1} s^{-1}. We thank Dr. Dennis Riley for these experiments.

Discussion

Catalase Mechanism. The initial lag phase for catalase activity starting with $LMn_2(CH_3CO_2)(ClO_4)_2$ involves an equilibrium with water, possibly by dissociation of the μ-acetate, as shown by the data of Figure 1 and Table 1. These data are interpreted as evidence for the first step of the proposed mechanism given in Scheme 2. Here an "active" form of the $Mn_2^{II,II}$ catalyst forms

(13) (a) Rush, J. D.; Maskos, Z. *Inorg. Chem.* **1990**, *29*, 897–905. (b) Larson, E. J.; Pecoraro, V. L. *J. Am. Chem. Soc.* **1991**, *113*, 7809–7810.
(14) Riley, D. P.; Rivers, W. J.; Weiss, R. H. *Ann. Biochemistry* **1991**, *196*, 344–349.

Scheme 2. Proposed Mechanism of Catalase Activity by $[LMn_2(CH_3CO_2)]^{2+}$

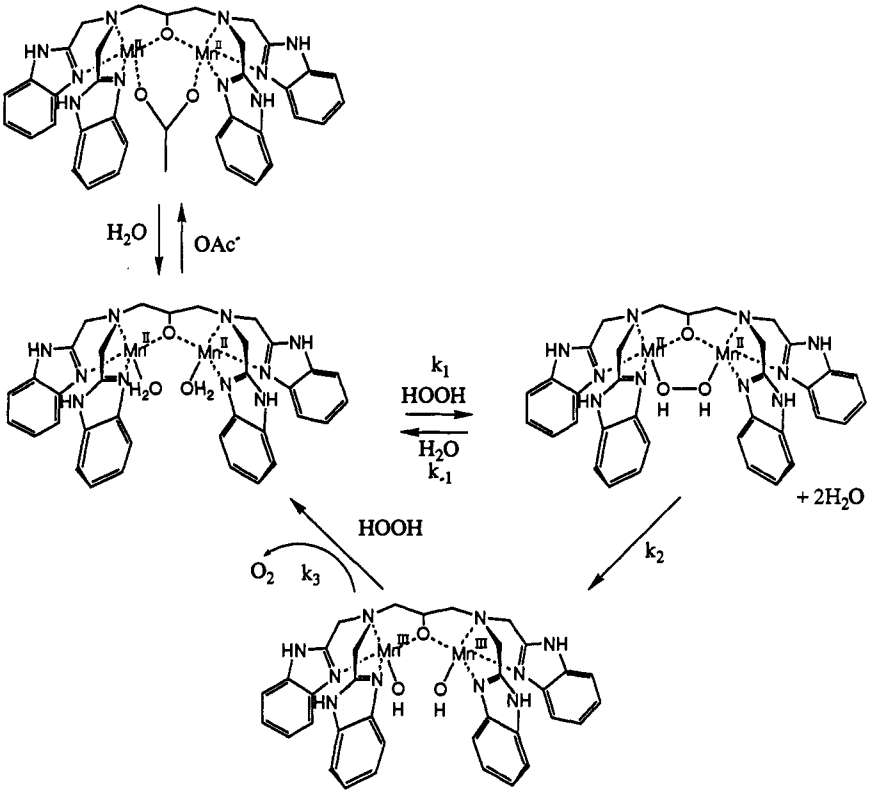

by dissociation of acetate in water to yield the $Mn_2^{II,II}(H_2O)_2$ species. This is favored by addition of water up to 2%. Hydrogen peroxide may bind to this "aqua" species in the second step by displacement of bound water, hence the competition observed above 2% water. The depicted mode of peroxide coordination, μ-$\eta^1\eta^1$ is not ascertained by the studies herein and may involve other stereochemistries. This is followed by intramolecular electron transfer in step four in which both Mn^{II} ions are oxidized to Mn^{III} concomitant with peroxide reduction to hydroxide. This is the rate-limiting step according to the optical data in Figure 5. Subsequent reduction by a second peroxide molecule would yield the O_2 product and restore the active starting material. The predicted steady-state rate expression expected for this mechanism under conditions of rapid preequilibrium with peroxide is given by eq 1.

$$\frac{\partial[O_2]}{\partial t} = \frac{k_1 k_2}{k_{-1}}[LMn_2^{II,II}][H_2O_2] \qquad (1)$$

This agrees with the experimentally observed rate expression, with $k_{obs} = k_1k_2/k_{-1}$ 0.23 M^{-1} s^{-1} at 297 K. In agreement with eq 1, the data in Figures 2 and 3 indicate that after the initial lag phase the steady-state rate of O_2 production from $LMn_2(CH_3CO_2)](ClO_4)_2$ is first-order in both reactants.

Although the simplest description of the active form of the catalyst describes this as an aqua species with the acetate fully dissociated, we cannot eliminate the possibility that the mode of acetate binding merely changes from bridging to monodentate, for example. We have found by EPR that if we start with an acetonitrile solution of **1** and titrate with tetra-*n*-ethylammonium acetate the EPR spectrum is converted to one which resembles that observed for an acetonitrile solution of the synthesized derivative $LMn_2(CH_3CO_2)_3$. We take this as evidence for inhibition by binding of a second μ-acetate. This is readily possible since both Mn ions in **1** are five-coordinate in solution. This offers a simple explanation for inhibition of the enzyme activity which occurs upon binding of a number of anions, including acetate, in the $MnCat^{II,II}$ oxidation state.[2b,c,f,3b]

The electronic absorption data in Figure 4 and the EPR data in Figure 6 point to formation of a colored, EPR-silent intermediate which occurs in parallel with the lag phase for catalase activity. This species reacts with excess peroxide in a catalytic process to evolve O_2, restore the $Mn_2^{II,II}$ EPR signal, and bleach the visible absorption (Figure 5). The electronic spectrum (λ_{max} = 425, 472, 760 nm) resembles that obtained for the EPR silent oxidized state of manganese catalase itself (λ_{max} = 400, 460, 500 nm), attributed to $Mn_2^{III,III}$,[2c] and also that observed for synthetic dimanganese^{III,III} complexes possessing the μ-*O*-di-μ-carboxylate linkage (486, 521, 720)[6a] (486, 503, 760 nm).[6b] The rates of the oxidative and reductive processes are solvent dependent, favoring a higher steady-state yield of oxidized species in protic solvents like methanol vs acetonitrile.

The mechanism in Scheme 2 is further supported by the data in Figure 5 showing that the ratio of concentrations of the $Mn_2^{III,III}$ intermediate to the catalyst concentration is a constant independent of time in the steady state. Applying the steady-state approximation to the intermediates in Scheme 2 predicts that this ratio is equal to a constant, given by eq 2

$$\frac{Mn_2^{III,III}}{Mn_2^{II,II}} = \frac{k_1 k_2}{k_3(k_{-1} + k_2)} \qquad (2)$$

where the rate constants are defined in Scheme 2.

The ratio of the final to steady-state absorptions in Figure 5 for the colored intermediate is about 7–9:1 in methanol. We interpret this to mean that the rate of reduction of the intermediate is about 7–9-fold faster than is oxidation to form the colored intermediate. In the steady-state region, there is no evidence for formation of either $Mn_2^{II,III}$ or $Mn_2^{III,IV}$ species under conditions of catalytic dismutation of peroxide.

We have previously measured the rate of catalase activity in the presence of one-to-one mixture of ligand, (HL) and Mn^{II} ions and found no catalase activity.[12] These results combined with our new results indicate that the dinuclear center is essential for catalase activity.

Another possibility for the mechanism would be to attribute the observed catalase activity to the minor uncoupled Mn^{II} species formed during turnover, as seen by EPR in Figure 6. This represents less then 5% of the starting material. The observation that this Mn^{II} species disappears at the end of the reaction and can be restored reversibly with more peroxide, indicates that it is not an irreversible decomposition product. An interesting hypothesis is that this species may represent intramolecular dismutation of the peroxide intermediate to form Mn^{II} and Mn^{IV}=O manganyl species, as depicted by eq 3. However, EPR spectroscopy did not reveal formation of an uncoupled Mn^{IV} species, as would be required if the Mn^{II} species is EPR detectable as an uncoupled monomeric center. Hence, the minor Mn^{II} species observed in acetonitrile may not be required for catalase activity.

$$LMn_2^{II,II}(H_2O)_2(H_2O_2) \rightarrow LMn_2^{III,III}(OH)_4 + 2H^+ \Leftrightarrow LMn^{II}(OH)_2Mn^{IV}{=}O + H_2O \quad (3)$$

A mechanism similar to that shown in eq 3 has been proposed recently for a synthetic $Mn_2^{II,II}$ complex, $LMn_2(\mu\text{-}PhCO_2)_2(NCS)$, which possess the five-coordinate ligand 2,6-bis{*N*-[[2-(dimethylamino)ethyl]imino]methyl}-4-methylphenolate.[15] The reaction with H_2O_2 produces Mn^{IV} and convincing evidence was given from FAB mass spectrometry and electronic spectroscopy for formation of two stable reaction products involving Mn^{II}-Mn^{IV}=O and $\{Mn^{IV}{=}O\}_2$ within an intact core possessing both μ-carboxylates and the μ-phenolate. Although kinetic data were not reported, which is essential to clarifying if these species are intermediates in catalysis or products of side reactions, it would appear these authors favor the former interpretation. The former species was proposed to form via oxidation of a $Mn^{II}Mn^{III}(OH)$ intermediate produced from a dimer possessing an intermolecular bridged μ-peroxo, $\{Mn^{II}Mn^{III}(PhCO_2)_2\}_2(\mu\text{-}O_2^{2-})$. The latter species was proposed to form via a $\{Mn^{III}(OH)\}_2$ intermediate from the intramolecular μ-peroxo species $Mn^{II}Mn^{III}(\mu\text{-}O_2^{2-})(PhCO_2)_2$. Thus in both cases the mechanism may involve redox cycling between Mn^{III} and Mn^{IV} for the catalase activity. The reason for formation of the Mn^{IV} oxidation state may be due to the different ligands relative to the ligand used in our complex, HL. A stronger ligand field is presented by the phenoxide + tertiary amine + bis(carboxylate) compared to the weaker ligand field of the alkoxo + bis(aromatic amine) + mono(carboxylate) in HL. Thus, comparison of these two classes of catalase mimics provides a clear illustration of the importance of ligand field strength in determining the accessible redox states which may participate in catalysis. $Mncat^{III,IV}$, which is inactive as a catalase, is believed to possess a strong six-coordinate ligand field provided by carboxylato and $(\mu\text{-}O)_2$ ligands, but no evidence has been found for a terminal oxo atom or for formation of the $MnCat^{IV,IV}$ state.[3c,8]

(15) (a) Sakiyama, H.; Tamaki, H.; Kodera, M.; Matsumoto, N.; Okawa, H. *J. Chem. Soc., Dalton Trans.* **1993**, 591–595. (b) Sakiyama, H.; Okawa, H.; Isobe, R. *J. Chem. Soc., Chem. Commun.* **1993**, 882–884.

Could a thermodynamic limitation explain the 7–9-fold slower kinetics of oxidation of the catalyst vs the reductive phase? Equations 4a and 4b give the two-electron half reactions for peroxide oxidation to O_2 and reduction to water at pH 7. Our electrochemical results on **1** indicate that formation of the $Mn_2^{III,III}$ state requires about 1.05 V in acetonitrile (vs NHE).[11] From this we see that coupling the unfavorable substrate oxidation reaction in eq 4a to reduction of the $Mn_2^{III,III}$ catalyst yields a favorable overall process by 0.77 V. Similarly, the unfavorable catalyst oxidation reaction would be coupled to the strongly favored reduction of peroxide in eq 4b to yield a favorable process by 0.30 V. In this way neither the oxidative nor reductive reactions would be thermodynamically disfavorable, and so may not impose kinetic limitations, provided the essential proton donors and acceptors noted in eqs 4b and 4a, respectively, are available. Although redox measurements are not available for the enzyme, the $MnCat^{II,II}$ oxidation state is known to undergo spontaneous oxidation in air at alkaline pH to yield $MnCat^{III,III}$.[2] This indicates a reduction potential which must be substantially smaller than the 1.05 V potential observed for $Mn_2^{III,III}$.

$$H_2O_2 \rightarrow O_2 + 2e^- + 2H^+ \qquad E_{1/2} = -0.28 \text{ V, pH 7} \quad (4a)$$

$$H_2O_2 + 2e^- + 2H^+ \rightarrow 2H_2O \qquad E_{1/2} = 1.35 \text{ V, pH 7} \quad (4b)$$

In the wet solvents we employed in this study, water should be functioning as both the proton donor and acceptor. Since $pK_w > 14$ for water in both acetonitrile and methanol, this is both a poor source of protons and a poor acceptor. By contrast, the active site of the catalase enzyme from *T. thermophilus*, possesses an essential proton donor with $pK_a \sim 11$ and an essential proton acceptor with $pK_a \sim 5.5$.[2f] These are presumed to represent protein residues involved in the delivery and removal of the two protons required for reduction and oxidation of substrate, respectively. Accordingly, the lack of low-energy proton donor and proton acceptor groups near to the catalytic site may be the principal reason for the 10^7-fold rate suppression of **1** compared to the enzyme.

Complex **1** and its derivatives appear to be the closest biomimetic examples of the dimanganese catalase enzymes. Although other Mn complexes exhibit catalase activity, where these have been investigated their mechanisms have been found to not mimic the MnCat enzymes.[13]

Acknowledgment. We thank Dr. S. V. Khangulov for thoughtful comments and Dr. Dennis Riley for SOD kinetic measurements. Research was supported by the National Institutes of Health (GM39932).

Note Added in Proof: After this manuscript was submitted a communication was published that also presented a manganese catalase mimic (Pecoraro et al. *J. Am. Chem. Soc.* **1993**, *115*, 7928).